

Purification phase transition in the central spin model: second Rényi entropy in dual space approach

V. V. Belov^{1,2}, W. V. Pogosov^{1,3,4,2}

¹*Dukhov Research Institute of Automatics (VNIIA), Moscow, 127030, Russia*

²*HSE University, Moscow, Russia*

³*Advanced Mesoscience and Nanotechnology Centre,
Moscow Institute of Physics and Technology (MIPT), Dolgoprudny, 141700, Russia and*

⁴*Institute for Theoretical and Applied Electrodynamics,
Russian Academy of Sciences, Moscow, 125412, Russia*

We conduct a numerical investigation of the dynamics of the central spin model in the presence of measurement processes. This model holds promise for experimental exploration due to its topology, which facilitates the natural distinction of a central particle and the quantum bath as different subsystems, allowing for the examination of entanglement phase transitions. To characterize the measurement-induced phase transition in this system, we employ a recently developed method based on second Rényi entropy in dual space. Our simulations account for decoherence, energy relaxation, and gate errors. We determine critical measurement rates and demonstrate that they significantly differ from those predicted by a simple approach based on mutual entropy.

PACS numbers:

I. INTRODUCTION

In recent years, there has been a surge of interest in exploring novel methodologies to mitigate quantum errors, with particular emphasis on the nascent domain of measurement-induced phase transition (MIPT). This emerging field offers promising avenues for error suppression in quantum systems. At its core, MIPT operates on a fundamental principle: while unitary operations generally enhance the entanglement degree of a system, measurements, conversely, tend to diminish it. For instance, the entanglement of two qubits can be achieved through unitary operations; however, the act of measuring one of the qubits results in the decoupling of their states.

The primary inquiries in the realm of MIPT revolve around elucidating the behavior of systems comprising numerous qubits subjected to entangling unitary operations and random quantum measurements. The interplay between entangling unitary evolution and disentangling measurements can give rise to highly intricate dynamics, including phase transitions between different states of entanglement. These transitions depend upon factors such as the frequency or intensity of measurements taken [1–11]. Various types of MIPT are discerned based on the system's initial state [1, 2, 4]. For mixed initial states, MIPT is commonly referred to as a purification phase transition. At low measurement rates, an entanglement phase predominates, characterized by an initial decrease in entanglement followed by stabilization at a nonzero level. Conversely, exceeding a critical measurement rate leads to a transition to the disentangling phase, where entanglement exponentially diminishes over time.

Recent experimental investigations of MIPT have been conducted using systems comprising superconducting qubits [12] and ion qubits [13].

The existence of MIPT was initially elucidated through approaches based on mutual entropy or Von Neumann entropy [2, 4]. However, recent studies have introduced a new method based on Rényi entropy, which offers clear advantages by providing a more direct measure of entanglement degree.

In this paper, we investigate the dynamics of the central spin model [14, 15] utilizing an approach based on second Rényi entropy with postselection derived from the generalized Lindblad equation in dual space. This spin system is well-suited for experimental exploration, as it comprises a single spin surrounded by a quantum bath of spins, with the central spin serving as a natural subsystem for determining entanglement entropy. Moreover, the symmetry of

the central spin model facilitates significant simplifications in calculations, enabling a greater number of qubits to be explored in numerical computations compared to other spin models. We employ second Rényi entropy as an indicator of phase transitions while analyzing entanglement between the central spin (qubit) and the remainder of the system. Our investigations also consider the effects of decoherence, energy relaxation, and gate errors, which are inevitable in real-world experiments. We assess their influence on the critical measurement rate and demonstrate that typical values of these parameters, characteristic of modern experimental setups, do not significantly suppress this quantity.

The paper is organized as follows. Section II defines the system under study. Section III formulates the method based on mutual entropy. Section IV presents an advanced approach based on second Rényi entropy. Section V analyzes the impact of gate errors, decoherence, and energy dissipation. We conclude in Section VI.

II. HAMILTONIAN AND PRELIMINARIES

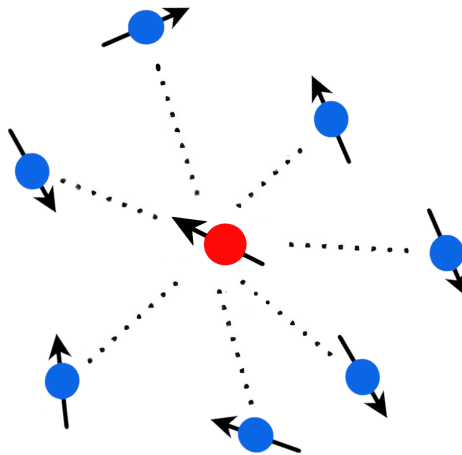


Fig. 1: Schematic image of the system described by the central spin model. Central 1/2-spin particle is interacting with the quantum bath of other spin-1/2 particles, which do not interact among themselves.

We consider a central spin model [14, 15], which describes a spin system shown schematically in Fig. 1. The spin (qubit) system is represented by a central spin interacting with the quantum "bath" of other spins, which do not interact directly with each other. The system Hamiltonian is given by

$$H = g \sum_{j=1}^L (\sigma_c^+ \sigma_j^- + \sigma_c^- \sigma_j^+) + \epsilon_c \sigma_{c,z} + \sum_{j=1}^L \epsilon_j \sigma_{j,z}, \quad (1)$$

where $\sigma_{j,z}$ and σ_j^\pm are Pauli operators associated with particles of the bath, while $\sigma_{c,z}$ and σ_c^\pm refer to the central spin; ϵ_j and ϵ_c are excitation energies of spins of the bath, whereas g is the interaction constant between the central spin and each spin of the bath, L is the number of spins in the bath. Hereafter we assume that $\epsilon_j = \epsilon_c$ for all j .

We switch to the rotating frame, in which there is only one energy scale associated with g . Then, we introduce a dimensionless system of units, in which the energy is measured in terms of g , while time is measured in terms of $1/g$.

III. PHASE TRANSITION MODEL BASED ON MUTUAL ENTROPY

Let us start by examining the description of phase transition dynamics based on the concept of mutual entropy, which is technically simpler compared to the approach using Rényi entropy. In practical applications, measurements

can be viewed as a quantum channel $\xi(\rho_{SE}(0), t)$ defined as [16–18]:

$$\rho_S(t) = \text{Tr}_E(U_{SE}(t)\rho_{SE}(0)U_{SE}^\dagger(t)) = \xi(\rho_{SE}(0), t), \quad (2)$$

where ρ_S refers to density matrix of the system under the study, ρ_E is the density matrix of the medium in which measurements are performed, and U_{SE} is the system plus environment evolution operator.

Next, we obtain the generalized Lindblad equation, which is used to describe the dynamics. Of crucial importance is the Kraus representation, which enables us to describe the system's state evolution through a set of operators known as Kraus operators. The Kraus representation establishes a relationship between the density matrix at time $t + \delta t$ and the density matrix at time t . It can be expressed as:

$$\rho_s(t + \delta t) = \sum_k \hat{A}_k \rho_s(t) \hat{A}_k^\dagger = \xi(\rho_s), \quad (3)$$

where \hat{A}_k are Kraus operators. Thus, the dynamics arise from the action of the quantum channel, which ensures fundamental physical principles such as probability conservation.

The expression for the density matrix at $t + \delta t$ is given by [16–18]:

$$\rho_s(t + \delta t) = \gamma \delta t \sum_k \hat{A}_k \rho_s(t) \hat{A}_k^\dagger + (1 - \gamma \delta t)(\rho_s(t) - i[H, \rho_s]\delta t) + O(\delta t^2), \quad (4)$$

where γ represents the measurement degree. If each qubit is measured sequentially no more than once, γ can be interpreted as the probability of qubit measurement per unit of time. The first term on the right-hand side of Eq. (4) describes the effect of measurement, while the second term is responsible for the unitary evolution. Specifically, since measurements occur with a probability of $\gamma \delta t$, it implies that with the opposite probability $(1 - \gamma \delta t)$, the system will undergo the usual unitary evolution.

In the limit $\delta t \rightarrow 0$, we derive the generalized Lindblad equation [19, 20]:

$$\frac{\partial \rho}{\partial t} = -[H, \rho(t)] + \gamma \sum_{a=1}^{L+1} [\hat{L}_a \rho(t) \hat{L}_a^\dagger - \frac{1}{2} \{\hat{L}_a^\dagger, \hat{L}_a \rho(t)\}], \quad (5)$$

where L_a represents the Lindblad operators or "jump" operators. If measurements are not performed on all qubits of the system, it is necessary to ensure trace preservation and Hermiticity for the Lindblad equation to be correct. Incomplete measurements are required because otherwise, postselection would be necessary after all experiments, leading to an exponentially increasing number of measurements [21]. To ensure that Eq. (5) preserves the trace of the matrix, we normalize the second term on the right-hand side of this equation and obtain:

$$\frac{\partial \rho}{\partial t} = -[H, \rho(t)] + \gamma \sum_{a=1}^m \frac{\hat{L}_a \rho(t) \hat{L}_a^\dagger}{\text{Tr}(\sum_{b=1}^m \hat{L}_b \rho(t) \hat{L}_b^\dagger)} - \frac{\gamma}{2} \sum_{a=1}^n \{\hat{L}_a^\dagger, \hat{L}_a \rho(t)\}, \quad (6)$$

where m ($m < L + 1$) represents the number of qubits that are measured.

Understanding the evolution of the density matrix enables us to calculate the entropy, which serves as a reflection of the system's phase. Investigating entanglement between two subsystems, namely the single qubit and the rest of the qubit system, is particularly advantageous for experimentally reproducing and analyzing the presence or absence of an entanglement phase transition [13]. However, the second Rényi entropy, defined as $S^{(2)} = -\log(\text{Tr}[\rho_A^2])$, fails to adequately describe this transition. The primary reason for this limitation is that this entropy also incorporates the probability distribution from different measurements. This aspect is discussed in more detail in Refs. [18, 22, 23]. In Section IV, we further discuss this issue.

Given the constraints of the second Rényi entropy, the metric for characterizing the phase transition can be the

mutual entropy S_{mutual} of the two subsystems [24, 25]. In Ref. [24], mutual entropy was utilized for this purpose due to the simplicity of such an approach, which provides an upper estimate for the critical value. Indeed, mutual entropy quantifies the shared information between the subsystems under consideration, making this description more closely related to information quantification [26].

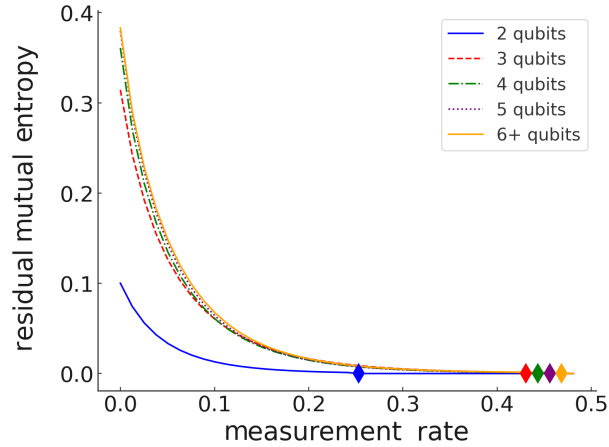


Fig. 2: Residual mutual entropy after the free evolution over $t = 15$ (in dimensionless units) as a function of the measurement rate in systems with varying numbers of qubits. The rhombus marks the critical point of transition from the mixed phase at lower γ to the pure phase at higher γ .

In the straightforward scenario where measurements are considered as instantaneous projections onto specific quantum states, Lindblad operators can be expressed as:

$$\begin{aligned}\hat{L}_{i,0} &= \frac{1}{\sqrt{N}}|0\rangle_i\langle 0|, \\ \hat{L}_{i,1} &= \frac{1}{\sqrt{N}}|1\rangle_i\langle 1|,\end{aligned}\tag{7}$$

where $i = 1, 2, \dots, L + 1$ and $N = 2^{L+1}$. For more complex measurement scenarios, it may be necessary to employ advanced methods described in Refs. [27, 28]. In our study, the quantum system and its dynamics are modeled using the Qutip library [29, 30]. Analyzing the entropy of a system involves examining its temporal evolution to ascertain whether the entropy has reached a saturation value (residual entropy) or has entirely disappeared. This approach facilitates the evaluation of the stability of the system state and the presence of phase transitions. For this analysis, the system's state after free evolution for $t = 15$ (in dimensionless units) is chosen, as saturation is observed at this stage. Random mixed initial states are employed to observe the purification phase transition [1, 4]. The results depicting mutual entropy versus measurement rate γ for different numbers of qubits are presented in Fig. 2. Beginning with a system comprising six qubits, the curves start to overlap, indicating that the system size no longer affects the critical measurement rate.

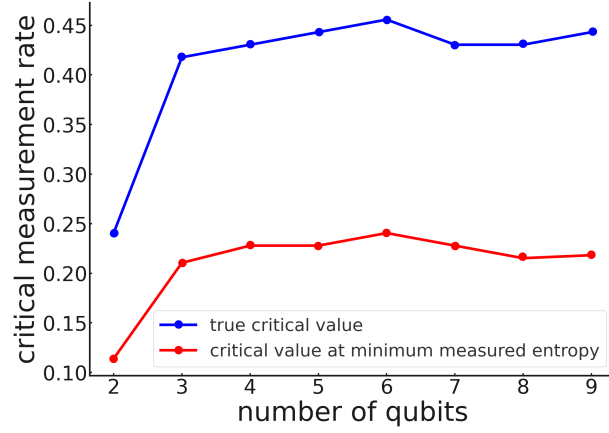


Fig. 3: Dependence of the critical value on the number of qubits using the approach based on mutual entropy. The upper graph illustrates the actual dependence of the critical value on the system size, while the lower one is calculated assuming that the minimum measurable entropy is approximately 10^{-3} . Solid curves serve as guides for eyes connecting discrete points.

As depicted, the critical measurement rate corresponding to the transition to the entanglement state increases with the system size. This arises from the fact that in smaller systems, even a single qubit measurement can significantly diminish the level of entanglement. However, as the system size increases, it is anticipated that the impact of individual measurements on the overall entanglement will diminish, and the critical value should converge to a saturation limit, denoted as P_{crit} , which no longer depends on the system size and is approximately 0.22. Additionally, it is observed that starting from a system of 9 qubits, the critical value reaches saturation. However, the deviation is sufficiently small to not warrant further investigation.

IV. APPLICATION OF THE GENERALIZED LINDBLAD EQUATION IN A DUAL SYSTEM

In the realm of quantum systems dynamics, it has become evident that the second Rényi entropy, when applied to an original system, does not consistently capture the intricacies within the system, particularly concerning entanglement phase transitions. However, recent studies [18, 22, 23] propose that by employing the concept of a doubled system and leveraging the properties of Einstein-Podolsky-Rosen (EPR) pairs, the necessary entropy can be correctly introduced, thereby circumventing the influence of the measurement probability distribution on the second Rényi entropy.

In this scenario, the original equation (6) is transformed into a generalized Lindblad equation for the dual system as:

$$\frac{\partial \rho_D}{\partial t} = -[H_D, \rho_D(t)] + \gamma \sum_{a=1}^m \frac{\hat{L}_{a,L} \hat{L}_{a,R} \rho_D(t) \hat{L}_{a,L}^\dagger \hat{L}_{a,R}^\dagger}{\text{Tr}(\sum_{b=1}^m \hat{L}_{b,L} \hat{L}_{b,R} \rho_D(t) \hat{L}_{b,L}^\dagger \hat{L}_{b,R}^\dagger)} - \frac{\gamma}{2} \sum_{a,b=1}^n \{\hat{L}_{a,L} \hat{L}_{a,R} \hat{L}_{b,L} \hat{L}_{b,R}, \rho_D(t)\}, \quad (8)$$

where $\rho_D = \rho \otimes \rho$, $H_D = H \otimes I + I \otimes H$, A and B are subsystems (in our case A contains L qubits, while B is represented by a single qubit). Then we can calculate the second Rényi entropy without probability distribution of measurements as

$$S_D = -\log_2(\text{Tr}_{L_A, R_A}[X_A \text{Tr}_{L_B, R_B}(\rho_D)]). \quad (9)$$

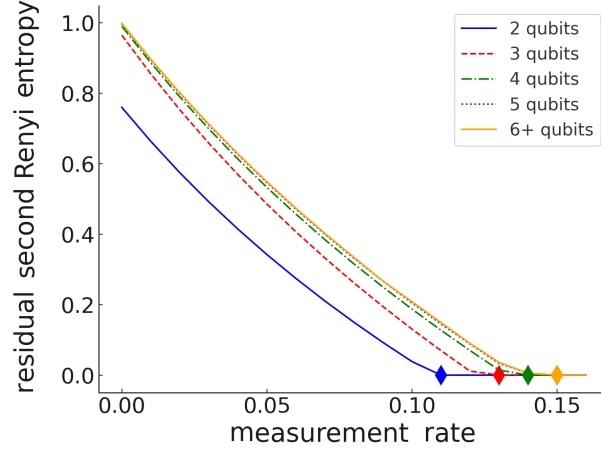


Fig. 4: Residual second Rényi entropy after the free evolution during the time $t = 15$ (in dimensionless units) as a function of the measurement rate in systems with different numbers of qubits. The rhombus shows the location of the critical point of transition from the mixed phase at lower γ to the pure phase at larger γ .

During the analysis of the dynamics of the double quantum system, particular attention is given to the normalization element, especially the element responsible for maintaining the unit trace of the density matrix. This attention stems from the fact that unlike in simpler models, the normalization element in the doubled system exhibits nonlinear characteristics.

To model the dynamics of the doubled system, we once again employ the Qutip library [29, 30]. Simulations can be conducted for either a pure or mixed initial state of the system, with the choice of initial state determining different types of measurement-induced phase transitions (MIPT) [1, 4]. As previously, we select a random mixed state as the initial state of the system to study the dynamical purification phase transition. The resulting dependencies of the residual entropy on the measurement rate are presented in Fig. 4.

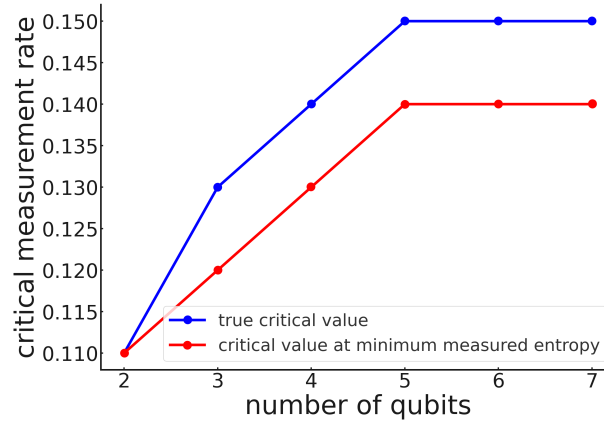


Fig. 5: Dependence of the critical measurement rate on the qubit number in a double system. The upper graph corresponds to the actual dependence of the critical value, while the lower one is calculated under the assumption that the minimum measurable entropy is approximately 10^{-3} . Solid curves serve as guides for eyes connecting discrete points.

As evident from Figs. 3 and 5, the second Rényi entropy yields critical values that differ from those obtained using the mutual entropy method. It stabilizes at a constant value with fewer qubits (as early as 5 qubits), unlike mutual entropy, which stabilizes at 9 qubits. The critical value for mutual entropy, under the condition of bounded entropy measurement, is approximately 0.22, whereas for the second Rényi entropy, it is approximately 0.14. Rényi entropy and mutual entropy offer distinct approaches to estimating entanglement and information distribution within

the system, resulting in varying critical value estimates. Mutual entropy quantifies the total shared information between two subsystems, providing an estimation of how much information about one subsystem's state influences the other. It is sensitive to changes in the entanglement structure as a phase transition approaches, characterized by significant shifts in information distribution within the system. Rényi entropy represents a broader class of measures for analyzing the probability distribution of states in a system and is more suitable in the vicinity of critical points.

The second Rényi entropy can more accurately capture critical changes in entanglement during MIPT due to its sensitivity to shifts in the distribution of eigenvalues of the state density matrix. On the other hand, mutual entropy may not fully capture these critical changes, as it focuses on quantifying information rather than qualitatively describing changes in the entanglement structure.

V. THE IMPACT OF GATE ERRORS, ENERGY RELAXATION, AND DECOHERENCE

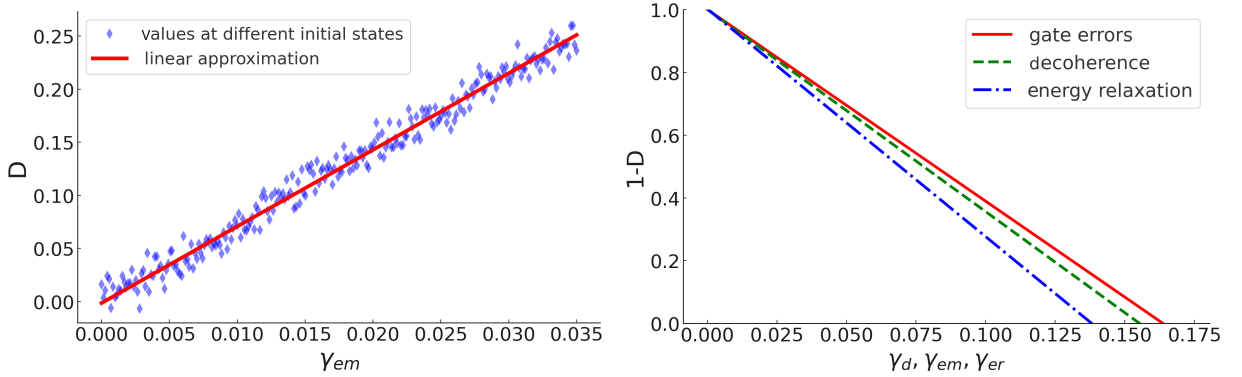


Fig. 6: (a) The relative decrease of the entropy D as a function of the energy relaxation constant. Each point corresponds to a different initial random mixed state. The straight line corresponds to the average dependence. (b) $1-D$ as a function of energy relaxation rate, decoherence rate, and gate error rate.

Gate errors, energy relaxation, and decoherence can significantly influence the dynamics of quantum systems, impacting both the evolution of unitary entanglement and the accuracy of measurements. Understanding the criticality of these factors is essential, as MIPT is expected to be utilized for quantum error correction. Errors can lead to unexpected changes in the system's state, reducing the efficiency of entanglement evolution and decreasing measurement accuracy. Energy relaxation, on the other hand, can diminish the overall level of entanglement in the system, thereby affecting the observability of phase transitions.

In the following, we will focus solely on the second Rényi entropy, although the influence of these negative effects will be analogous for mutual entropy. In the simplest case of the Markov approximation, where the 'reservoir' relaxation is fast and the interaction is weak, all these effects can be described through additional Lindblad operators [31, 32]. While more general methods are available [27, 33], the results remain practically unchanged. The Lindblad operators for each of the main negative processes are: decoherence is described by $L_{rel} = \sqrt{\gamma_d}\sigma^z$, energy relaxation by either $L_{em} = \sqrt{\gamma_{em}}\sigma^+$ or $L_{abs} = \sqrt{\gamma_{abs}}\sigma^-$, and gate errors by $L_{er} = \sqrt{\gamma_{er}}\sigma^y$ or $\sqrt{\gamma_{er}}\sigma^x$. We then substitute these additional Lindblad operators into Eq. (8). We model each of these effects separately and present the results in Fig. 6. Essentially, the effect of gate errors, energy relaxation, and decoherence is to shift all graphs in Fig. 4 to the left. Specifically, the critical value decreases due to these effects. Figure 6 (a) illustrates the relative decrease of the entropy D as a function of the energy relaxation constant, exhibiting a linear behavior. Each point corresponds

to a different initial random mixed state. The solid line provides an averaged linear approximation for D versus γ_{em} . Figure 6 (b) shows $1 - D$ as a function of the energy relaxation rate, decoherence rate, and gate error rate. Similar average linear dependencies, as in Fig. 6 (a), are plotted. We observe that all three dependencies are linear, and the critical value vanishes at approximately the same value of these rates.

The simulations demonstrate that in experiments, we can achieve a regime where entanglement prevails, provided that g is one or two orders of magnitude larger than γ_i . This requirement is realistic, for instance, for superconducting physical platform. The largest negative influence is exerted by the energy relaxation process, while the smallest is by quantum gate errors.

VI. CONCLUSIONS

In this study, we examined MIPT for the central spin model, which characterizes a single two-level particle interacting with a quantum bath composed of other two-level systems. This model is pertinent for describing phenomena observed in quantum dots and defect centers in diamond. In the realm of MIPT, the central spin model holds promise for experimental quantum simulation using artificial quantum systems like superconducting qubits, owing to its topology that naturally segregates the central particle from its quantum bath.

We determined the critical measurement rate marking the transition from one phase to another using two approaches: (i) the conventional method based on mutual entropy and (ii) a recently proposed theoretical framework based on the second Rényi entropy in dual space. Our findings revealed that both approaches exhibit similar tendencies, yet the second Rényi entropy approach yields a significantly smaller critical measurement rate.

Furthermore, we explored the impact of energy relaxation, decoherence, and quantum gate errors, all of which are inevitable in real-world experiments. Through numerical modeling, we assessed their effects and demonstrated the feasibility of observing MIPT in the central spin model within modern artificial quantum systems.

VII. ACKNOWLEDGMENTS

W. V. P. acknowledges support from the RSF grant No. 23-72-30004 (<https://rscf.ru/project/23-72-30004/>).

-
- [1] B. Skinner, *Lecture notes: Introduction to random unitary circuits and the measurement-induced entanglement phase transition* (2023), 2307.02986.
 - [2] B. Skinner, J. Ruhman, and A. Nahum, Phys. Rev. X **9**, 031009 (2019), URL <https://link.aps.org/doi/10.1103/PhysRevX.9.031009>.
 - [3] Y. Li, X. Chen, and M. P. A. Fisher, Phys. Rev. B **98**, 205136 (2018), URL <https://link.aps.org/doi/10.1103/PhysRevB.98.205136>.
 - [4] M. J. Gullans and D. A. Huse, Phys. Rev. X **10**, 041020 (2020), URL <https://link.aps.org/doi/10.1103/PhysRevX.10.041020>.
 - [5] E. Granet, C. Zhang, and H. Dreyer, Phys. Rev. Lett. **130**, 230401 (2023), URL <https://link.aps.org/doi/10.1103/PhysRevLett.130.230401>.
 - [6] G. Mazzucchi, W. Kozłowski, S. F. Caballero-Benitez, T. J. Elliott, and I. B. Mekhov, Phys. Rev. A **93**, 023632 (2016), URL <https://link.aps.org/doi/10.1103/PhysRevA.93.023632>.
 - [7] Y. Li, X. Chen, and M. P. A. Fisher, Phys. Rev. B **100**, 134306 (2019), URL <https://link.aps.org/doi/10.1103/PhysRevB.100.134306>.
 - [8] A. Chan, R. M. Nandkishore, M. Pretko, and G. Smith, Phys. Rev. B **99**, 224307 (2019), URL <https://link.aps.org/doi/10.1103/PhysRevB.99.224307>.

- [9] M. Szyniszewski, A. Romito, and H. Schomerus, Phys. Rev. B **100**, 064204 (2019), URL <https://link.aps.org/doi/10.1103/PhysRevB.100.064204>.
- [10] J. Hoke, M. Ippoliti, E. Rosenberg, D. Abanin, R. Acharya, T. Andersen, M. Ansmann, F. Arute, K. Arya, A. Asfaw, et al., Nature **622**, 481–486 (2023), URL <https://doi.org/10.1038/s41586-023-06505-7>.
- [11] I. Poboiko, I. V. Gornyi, and A. D. Mirlin, Phys. Rev. Lett. **132**, 110403 (2024), URL <https://link.aps.org/doi/10.1103/PhysRevLett.132.110403>.
- [12] M. Niknam, L. F. Santos, and D. G. Cory, Phys. Rev. Lett. **127**, 080401 (2021), URL <https://link.aps.org/doi/10.1103/PhysRevLett.127.080401>.
- [13] C. Noel, P. Niroula, D. Zhu, A. Risinger, L. Egan, D. Biswas, M. Cetina, A. V. Gorshkov, M. J. Gullans, D. A. Huse, et al., Nature Physics **18**, 760–764 (2022), URL <http://dx.doi.org/10.1038/s41567-022-01619-7>.
- [14] Y. Ashida, T. Shi, R. Schmidt, H. R. Sadeghpour, J. I. Cirac, and E. Demler, Phys. Rev. Lett. **123**, 183001 (2019), URL <https://link.aps.org/doi/10.1103/PhysRevLett.123.183001>.
- [15] A. A. Zhukov, S. V. Remizov, W. V. Pogosov, and Y. E. Lozovik, Quantum Information Processing **17**, 223 (2018), URL <http://dx.doi.org/10.1007/s11128-018-2002-y>.
- [16] J. D. Cresser, S. M. Barnett, J. Jeffers, and D. T. Pegg, Optics Communications **264**, 352 (2006), quantum Control of Light and Matter, URL <https://www.sciencedirect.com/science/article/pii/S0030401806004962>.
- [17] H. M. Wiseman and G. J. Milburn, *Quantum Measurement and Control* (Cambridge University Press, 2009).
- [18] Y.-N. Zhou, SciPost Phys. Core **6**, 023 (2023), URL <https://scipost.org/10.21468/SciPostPhysCore.6.1.023>.
- [19] C. Brasil, F. Fanchini, and R. Napolitano, Revista Brasileira de Ensino de Física **35** (2011).
- [20] Y. Cao and J. Lu, Journal of Mathematical Physics **58** (2017), URL <http://dx.doi.org/10.1063/1.4993431>.
- [21] A. J. Friedman, O. Hart, and R. Nandkishore, *Measurement-induced phases of matter require feedback* (2023), 2210.07256.
- [22] Y.-N. Zhou, L. Mao, and H. Zhai, Phys. Rev. Res. **3**, 043060 (2021), URL <https://link.aps.org/doi/10.1103/PhysRevResearch.3.043060>.
- [23] M. Buchhold, Y. Minoguchi, A. Altland, and S. Diehl, Phys. Rev. X **11**, 041004 (2021), URL <https://link.aps.org/doi/10.1103/PhysRevX.11.041004>.
- [24] Q. Tang and W. Zhu, Phys. Rev. Res. **2**, 013022 (2020), URL <https://link.aps.org/doi/10.1103/PhysRevResearch.2.013022>.
- [25] C. Cai and S. Verdú, Entropy **21**, 969 (2019).
- [26] M. Ozawa and N. Javerzat, *Perspective on physical interpretations of rényi entropy in statistical mechanics* (2024), 2404.06436.
- [27] H. Carmichael, *An Open Systems Approach to Quantum Optics* (Springer Berlin, Heidelberg, ???), ISBN 978-3-540-47620-7 Published: 17 February 2009, URL <https://doi.org/10.1007/978-3-540-47620-7>.
- [28] M. Scala, R. Migliore, and A. Messina, Journal of Physics A: Mathematical and Theoretical **41**, 435304 (2008), URL <http://dx.doi.org/10.1088/1751-8113/41/43/435304>.
- [29] J. Johansson, P. Nation, and F. Nori, Computer Physics Communications **183**, 1760 (2012), URL <https://www.sciencedirect.com/science/article/pii/S0010465512000835>.
- [30] J. Johansson, P. Nation, and F. Nori, Computer Physics Communications **184**, 1234 (2013), URL <https://www.sciencedirect.com/science/article/pii/S0010465512003955>.
- [31] W. Tarnowski, D. Chruściński, S. Denisov, and K. Życzkowski, Open Systems & Information Dynamics **30** (2023), URL <http://dx.doi.org/10.1142/S1230161223500075>.
- [32] M. Howard, J. Twamley, C. Wittmann, T. Gaebel, F. Jelezko, and J. Wrachtrup, New Journal of Physics **8**, 33–33 (2006), URL <http://dx.doi.org/10.1088/1367-2630/8/3/033>.
- [33] G. O. Samach, A. Greene, J. Borregaard, M. Christandl, J. Barreto, D. K. Kim, C. M. McNally, A. Melville, B. M. Niedzielski, Y. Sung, et al., Phys. Rev. Appl. **18**, 064056 (2022), URL <https://link.aps.org/doi/10.1103/PhysRevApplied.18.064056>.